ORIGINAL PAPER

PVA Based Ternary Nanocomposites with Enhanced Properties Prepared by Using a Combination of Rice Starch Nanocrystals and Silver Nanoparticles

S. Vasantha Kumar[1] · Johnsy George[1] · V. A. Sajeevkumar[1]

Abstract

Ternary nanocomposite films exhibiting better properties were prepared by incorporating two different nanoparticles such as rice starch nanocrystals (RSN) and silver nanoparticles (AgNPs) together in polyvinyl alcohol (PVA) matrix at various concentrations. The morphological evaluation using atomic force microscopy revealed that the particle size of RSN nanoparticles varied from 50 to 125 nm. The nanocomposite films made using these nanoparticles were evaluated for its chemical, mechanical and thermal properties. FTIR spectra of the films revealed some specific vibrational bands of RSN along with the characteristic bands of PVA. The mechanical property analysis of nanocomposite films indicated better tensile strength and elongation properties, which can be attributed to the strong interaction of PVA with RSN and AgNPs. The thermal properties of these films were also evaluated. These ternary nanocomposites exhibited superior mechanical properties, which is very much beneficial as far as the end use applications are concerned.

Keywords Polyvinyl alcohol · Starch nanocrystals · Silver nanoparticles · Ternary nanocomposite

Introduction

PVA is a synthetic polymer, which is biodegradable, biocompatible, easy to process and has good physical and chemical properties [1]. Since PVA consists of hydroxyl groups in its main chain, they are water-soluble too. Food packaging is one potential application area, where PVA can be extensively used for making environmentally friendly packaging systems that can reduce the negative impact of conventional, nondegradable polyolefin based packaging materials. The properties of PVA such as film-forming ability, biocompatibility, non-toxic nature, chemical resistance, thermal stability and clarity made it useful for food packaging and biomedical applications [2, 3]. Although PVA is having reasonably good properties, efforts are being undertaken to improve some of the mechanical properties to make it comparable with other commodity plastics. Improvement in the mechanical properties can be achieved by incorporating certain additives

and commonly used additives for this purpose are natural polymers like starch [4], cellulose [5], chitin and chitosan [6], proteins [7] etc. However, the simple blending of PVA with these fillers has shown to decrease its properties and even film forming characteristics was compromised due to the poor compatibility between PVA and the added fillers [8]. The advent of nano materials opened a new path to reinforce polymers such as PVA, as nanomaterials are capable of imparting novel properties to many polymers. Some of the nanometers, which were used along with PVA for this purpose include carbon nanotubes [9], graphene [10], carbon nano fibers [11], nanoclays [12], cellulose nanocrystals [13] etc. Similar to cellulose nanocrystals, the use of starch nanocrystals as reinforcing fillers in PVA was also reported [14]. The PVA nanocomposites made by incorporating these nanomaterials exhibit unique properties due to their nanometric size effect, better dispersion and probably due to the better physical as well as chemical interactions. However, the improvements in the properties of these polymer nanocomposites depend on various parameters such as the size, shape, aspect ratio, modulus of the nano particles as well as the extent of dispersion, alignment and interaction with the matrix in a nanocomposite [15].

✉ Johnsy George
  g.johnsy@gmail.com

[1] Defence Food Research Laboratory, Siddarthanagar, Mysore 570 011, India

Among the above-mentioned nanomaterials, nanoparticles derived from starch is one of the most promising nanomaterials for reinforcing PVA, because of its large-scale availability, renewability, low cost, biodegradability and the possibility of chemical modifications. Naturally occurring starch consists of an annular structure of alternate layers of crystalline and semi-crystalline or amorphous regions [16]. The crystalline fractions of starch can be separated by acid hydrolysis, where acid preferentially attacks the amorphous regions of the starch, resulting in an increase in crystallinity [17]. As a result of acid hydrolysis, starch nanocrystals exhibiting high crystallinity and nanoscale morphology can be obtained. The nanocrystals obtained like this, have different size and shape, depending on the type of starch and the hydrolysis method employed [18]. Putaux et al. reported the preparation of platelet-like nanoparticles with a length and width of 20–40 nm and 15–30 nm respectively by the hydrochloric acid hydrolysis of waxy maize starch granules [19]. It is also reported that waxy maize starch granules subjected to sulfuric acid hydrolysis resulted in the formation of grape-like aggregates composed of crystalline platelets with round edges having an average diameter of 25–40 nm [20]. Acid hydrolysis was also employed in the synthesis of corn starch and potato starch nanocrystals having a size range of 70–100 and 9–20 nm respectively [21, 22]. Bigger starch nanocrystals having a length of 60–150 nm and a width of 15–30 nm were synthesised using sulfuric acid hydrolysis of pea starch [23]. The differences in the particle size and shape can be attributed to the botanical origin of starch, hydrolysis technique employed and due to the difficulties in obtaining well-defined images of non-aggregated starch nanocrystals.

Starch nanocrystals can assist in reinforcing several natural and synthetic polymers due to its special nano morphology, intrinsic rigidity and strong interfacial interactions. The nanocrystals also possess a number of hydroxyl groups that help to achieve miscibility and interfacial interactions with the hydrophilic polymer matrix. These types of enhanced miscibility and interfacial interactions are the main reasons for better mechanical performance exhibited by these polymer nanocomposites. Starch nanocrystals can also form a continuous percolating network within the polymer matrix held together by hydrogen bonding, which maximizes stress transfer and enhancing reinforcement [24]. PVA nano composites containing pea starch nanocrystals have been reported to produce materials with enhanced mechanical properties, higher light transmittance and lower moisture uptake. Due to their smaller size, these starch nanoparticles disperse more homogeneously in PVA and results in stronger interactions [14]. However, the reinforcing effect was comparatively lower with pea starch nanocrystal in the PVA matrix and the mechanical properties such as tensile strength and elongation at break reduced significantly as the nanocrystal concentration increased. As the percentage concentration of starch nanocrystal increased, they tend to self-aggregate and resulted in the formation of weak points that generally induces brittleness to the nanocomposite. Recently ternary nanocomposites that employ two different nanomaterials together in a single polymer matrix have been demonstrated to exhibit better mechanical properties [25]. The use of silver nanoparticles (AgNPs) along with cellulose nanocrystals helped to improve the elongation properties of these nanocomposites. The aim of the present study is twofold. First, it aims at the synthesis of rice starch nanocrystals (RSN) and to evaluate its efficacy in improving the properties of PVA compared to normal rice starch (RS) as studies on the efficacy of rice starch nanoparticles in reinforcing polymers such as PVA is less reported. Secondly, this study is aimed to assess the feasibility to fabricate ternary nanocomposite films with better mechanical properties using AgNPs as a co-additive along with RSN.

Materials and Methods

Materials

Rice grains (Sona Masuri, Chudi Brand) were purchased from Shrilaksmi Narashima Industries, Raichur, Karnataka, India. Sodium hydroxide (NaOH), sulphuric acid (H_2SO_4) and silver nitrate ($AgNO_3$) of analytical grade were procured from Sd fine chemicals, India. PVA (molecular weight—14,000) was supplied by Fisher Scientific India. Sodium borohydride ($NaBH_4$) was purchased from Sigma Chemical Co. USA.

Preparation of Rice Starch

Starch was isolated from rice grains by an alkali method which removes protein from it [26]. Rice grain was powdered and then steepened in 0.2% NaOH solution at room temperature for 24 h. The supernatant layer was decanted, and the slurry was diluted to the original volume with NaOH solution. The process was repeated until the supernatant becomes clear and gives a negative reaction to the Biuret test for protein. The RS thus obtained was suspended in distilled water, passed through 100–200 mesh nylon cloth and repeatedly washed with water until the pH of the supernatant was found to be around 7.0, measured using a pH meter (Eutech Instruments, Thermo Fisher Scientific, India). The RS was collected by centrifugation and later dried in an incubator (Appolo Scientific Surgical Co, India) at 40 °C. The total yield of RS obtained was 70–75% w/w.

Preparation of Rice Starch Nanocrystals

RSN was prepared as per the procedure previously reported by Angellier et al. [27]. About 15 g of RS was mixed with 250 mL of H_2SO_4 (3.14 M) solution in a round bottom flask. The suspension was maintained at 40 °C and continuously stirred at 180 rpm in an orbital shaker (Scigenics Biotech Pvt Ltd, India). After 7 days of acid hydrolysis, the suspensions were centrifuged. The precipitate was repeatedly washed with distilled water and centrifuged each time (Remi Elekrotechnik Ltd, India) until the suspension was neutral (confirmed using a pH meter). This resultant residue was lyophilized to get a fine powder of RSN.

Preparation of PVA Nanocomposite Film

PVA solution was prepared by dissolving 10 g PVA in 100 mL distilled water at 90 °C for 4 h with mechanical stirring. Different weight percentages of RS and RSN (2, 4, 6, 8 and10 wt%) were dispersed in a known weight of PVA solution (100 mL, 10 wt%). The solution was cast on a flat levelled non-sticky polymer surface and allowed to dry at room temperature to obtain films of uniform thickness. Ternary nanocomposite films consisting of starch nano crystals and silver nano particles were prepared by a two-step process. Initially, PVA solution was mixed thoroughly with the calculated quantity of RSN using a mechanical stirrer and to this solution, a calculated quantity of 1 mM $AgNO_3$ solution is added. Silver nanoparticles were synthesized in situ in this solution by the reduction of $AgNO_3$ using a very dilute solution of $NaBH_4$ (0.1 mol/L). The formation of silver nanoparticles was confirmed by observing its surface plasmon resonance using a UV–visible spectrometer. Ternary nanocomposite films were developed by casting and evaporation of the above solution using the same process described above. The film after vacuum drying at 40 °C was kept in a desiccator containing P_2O_5 before it was used for further analysis. All the films were conditioned at 50% RH for 7 days and were used for mechanical and thermal property evaluation.

Characterizations

The amount of amylose and amylopectin present in the RS and RSN samples were determined by the method reported by Williams et al. [28] using a UV–visible Spectrometer (Genesys 2, M/s Spectronic, Thermo Fisher Scientific, India) by observing its absorbance at the wavelength 620 nm. 0.1 g of the starch sample was taken in a beaker and 1 ml of 99% ethanol and 9 ml of 1 M NaOH solution was added and mixed well. This solution was heated to gelatinize the starch, in a boiling water bath for 10 min. After cooling, the solution was transferred to a 100 ml standard flask and made up to the mark using distilled water. About 5 ml of the above solution were taken in another 100 ml volumetric flask and mixed with 1.0 ml of 1 M acetic acid and 2.0 ml of Iodine solution. The absorbance of the above solution was measured using UV Visible spectrophotometer at 620 nm using water as blank and used for calculating the percentage composition of amylose and amylopectin. From the absorbance data, the percentage of amylose and amylopectin were calculated [28].

The X-ray diffractograms (XRD) of the RS and RSN samples were recorded using X-ray diffractometer (D2 Phaser, Bruker AXS, Germany) with Ni filter, operating at 30 kV and 10 mA. The diffraction patterns were recorded using CuKα radiation of wavelength λ = 1.5406 Å. The samples were scanned in the 2θ range 1°–40° with a scan speed of 5°/min and step size of 0.02. The percentage crystallinity was calculated using TOPAS™ software supplied along with the X-ray diffractometer. The morphological analysis of RS and RSN were carried out using Scanning Electron Microscopy (SEM) and Atomic Force Microscopy (AFM). SEM images of RSN samples were obtained using an EVO LS10 SEM (Zeiss, UK). The samples were initially dried in vacuum and placed on an aluminium stub using double-sided aluminium tape and sputter coated. The morphological analysis was carried out in high vacuum using an operating voltage of 20 kV. SEM was also used to analyse the morphology of nanocomposites films. The liquid nitrogen fractured surface of nanocomposite samples was prepared and their morphology was analysed. AFM analysis was carried out using a Solver PRO-M scanning probe microscope from NT-MDT, Ireland. For AFM analysis, a small amount of RSN was dispersed in distilled water and a drop of the suspension was dried overnight on a freshly cleaved mica substrate. The images were acquired using the non-contact mode with silicon cantilevers, having a tip curvature radius of 10 nm and a force constant of 1.45–15.1 N/m. Infrared spectra of all the samples were recorded using a Thermo Nicolet, FTIR Spectrometer (Model 5700), Madison, WI, USA by using single bounce ZnSe crystals. All the spectra were recorded in the mid IR range (4000–650 cm^{-1}) at 4 cm^{-1} resolution. 32 scans were averaged to get the IR spectra. IR spectra of some samples were measured in the absorbance mode from 4000–400 cm^{-1} with the same resolution for characterization of low-intensity bands. Mechanical properties of nanocomposite films were evaluated in the tensile mode using a Universal Testing Machine (UTM) (Lloyd Instruments, Model: LRX Plus), with a crosshead speed of 100 mm/min with a gauge length of 1 inch. All the samples were cut into strips with a length of 5 cm and a width of 1 cm as per ASTM D882 method. Ten different sample strips were used for mechanical property evaluation and the stress–strain graph of samples that comes close to average value was taken. Thermal analysis of the nanocomposite films was carried

Table 1 Percentage of amylose and amylopectin content in extracted rice starch and rice starch nanocrystals

Sample	Absorbance at 620 nm	Percentage of amylose (wt%)	Percentage of amylopectin (wt%)
Rice starch	0.386 ± 0.004	23.61 ± 0.24	76.39 ± 0.24
Rice starch nanocrystal	0.102 ± 0.003	6.24 ± 0.21	93.76 ± 0.21

out using Differential Scanning Calorimeter (DSC) and Thermogravimetric analyser (TGA). A DSC with a thermal analyst system (DSC 2910, TA Instruments, USA) was used to determine the glass transition temperature (T_g), melting temperature (T_m) and melting enthalpy (ΔH_m) of PVA and its nanocomposites films. Samples were scanned at a heating rate of 10 °C/min over the temperature range of −20 to 250 °C. Thermogravimetric analysis was carried out (TGA Q50, TA instrument, USA) to determine the thermal stability of PVA and its nanocomposites under nitrogen flow rate of 20 ml/min. The samples were heated from 30 to 600 °C with a heating rate of 10 °C/min. The percentage weight loss of the sample and derivative weight loss were plotted against the temperature of all the samples. The onset, peak and completion temperature were calculated using the software. Dynamic mechanical analysis (DMA) was performed on a dynamic mechanical thermal analyser (Model Q 800, TA instrument, USA). The measurements were carried out by applying a constant shear stress at a frequency of 5 Hz while fixing the static load at 4.0 N and dynamic load at 2.0 N respectively. The samples were prepared by cutting strips from the films and were tested at a temperature range of 25–80 °C by providing a heating rate of 5 °C/min. The storage modulus, loss modulus and tan δ of the samples were measured simultaneously using the instrument.

Results and Discussion

UV–Vis Analysis

The amount of amylose and amylopectin present in the RS and RSN samples were calculated from the absorbance data of UV–Vis spectroscopy and presented in Table 1. In the rice starch, the percentage of amylose was found to be around 24 wt%, but its percentage reduced to around 6 wt% as it gets converted to starch nanocrystals. Since amylose is a linear molecule with limited branching compared to amylopectin, they are highly susceptible to acid hydrolysis. During the acid hydrolysis, less crystalline fractions of amylose get hydrolysed and removed. This is evident from the results as shown in Table 1. The in-situ synthesis of AgNPs resulted in a bright yellowish coloured film, which implied the formation of silver nanoparticles. The UV–Vis absorption spectra of PVA–RSN nanocomposites containing
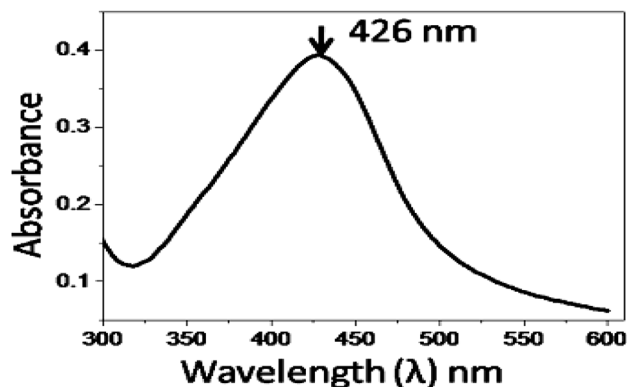
Fig. 1 UV–Vis absorption spectra of silver nanoparticle containing PVA–RSN nanocomposites
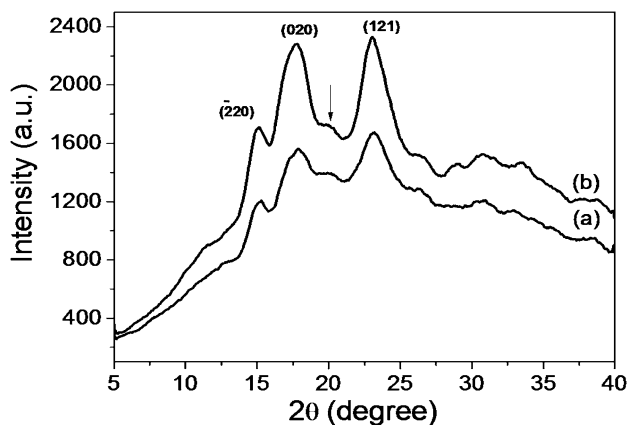
Fig. 2 XRD spectra of (*a*) extracted rice starch and (*b*) rice starch nanocrystals

silver nanoparticles show a characteristic surface plasmon resonance peak at 426 nm as shown in Fig. 1, confirms the formation of silver nanoparticles in the polymer matrix.

X-ray Diffraction Analysis

The X-ray diffraction pattern of RS and RSN is depicted in Fig. 2.

The diffraction pattern of both RS and RSN matches to the characteristic A-type crystalline pattern of rice starch with strong reflections at 2θ values of 17° and 23° [29]. The XRD pattern of RS also exhibited a weak intensity peak at

15.1° in addition to the strong intensity peaks at 17.8°, 23.1°. The peaks around 15.1°, 17.8° and 23.1° correspond to the diffraction peaks of ($\bar{2}$20), (020) and (121) *h, k, l* crystal planes [30]. The RSN samples also show similar peaks, but the intensity of peaks at 15.1°, 17.8° and 23.1° increased remarkably. This implies that the starch nanocrystals also inherited the original crystalline pattern of rice starch, but at the same time an increase in the intensity of peaks suggests that crystalline fractions become more prominent after hydrolysis. This is an indication that the overall crystallinity of the samples was increased after acid hydrolysis. During acid hydrolysis, acid attacks amorphous areas of starch rapidly compared to the crystalline region and hydrolyse them into small molecular weight fractions [31]. The crystalline fractions that are more resistant to acid hydrolysis due to their close packing nature do not allow acid to penetrate faster. If the hydrolysis process is carried out in such a way that only amorphous regions were selectively removed, then more acid resistant crystalline fractions can be retrieved [19]. These fractions are rich in crystalline domains and possess higher crystallinity. In our investigation, the crystallinity of rice starch and its nanocrystals obtained after acid hydrolysis was calculated by plotting a baseline that separates crystalline domains from amorphous areas. Gaussian line shapes were chosen for the curve fitting procedure as it produces reproducible results [30]. The ratio of the area above the baseline to the total area was taken as the percentage degree of crystallinity. For RS, the percentage crystallinity was calculated as 25.5%. After hydrolysis, the percentage crystallinity was increased to 48%, which suggests that some of the amorphous fractions were removed as a result of acid hydrolysis. The crystallinity of starch is mainly attributed to the close packing of amylopectin side chains that are arranged in double helices and will be able to pack into crystalline domains. In order to cross check the results, the amylose content in RS was experimentally calculated [32] and found to be 23.6%. After hydrolysis, amylose content was reduced to 6.2%, which suggests that as the amount of amylose reduces, the relative content of amylopectin in the starch sample increases, which contribute to the overall increase in the crystallinity. In addition to this, a broad diffraction background visible at 2θ around 11° got attenuated after hydrolysis, which also suggests the removal of some amorphous features of starch [33]. Another important observation is that a relatively weak peak at 2θ around 20° got altered after the acid hydrolysis. Lopez-Rubio et al. assigned this peak to a single helical conformation associated with the amylose–lipid complexes [30]. Hence a change in the peak position is an indication that the acid hydrolysis affected the amylose–lipid complexes also. During acid hydrolysis, lipids and proteins will get separated from the starch molecules and hence the amylose–lipid complexes were altered.

Morphological Characterization

SEM and AFM images of RS and RSN are given in Fig. 3.

RS granules were found to have pentagonal shape and possess a granular size of 6–7 µm (Fig. 3a), which is in agreement with earlier reports [34]. After hydrolysis, the particle size of rice starch significantly reduced and brought down to the nanometer scale. The size of these particles was found to be in the range of 50–125 nm, as evident from the AFM images (Fig. 3b). A representative size measurement using AFM is shown in Fig. 3c. After acid hydrolysis, more crystalline starch fractions which are in the domain of nanosize range can be retrieved. These nano particles were used for the preparation of nanocomposites by incorporating them in a polymer matrix such as PVA. The cross-sectional SEM images of PVA and its nanocomposites are shown in Fig. 3d–f. PVA has a relatively smooth surface (Fig. 3d), whereas its nano composites with RSN shows more roughness (Fig. 3e), which is an indication that some amount of aggregation of RSN, which has taken place within the nanocomposite. This may be due to the fact that the interaction between starch nanoparticles and PVA are relatively weak in nature and RSN particles tend to aggregate within the polymer matrix. On the other hand, the addition of silver nanoparticles along with RSN contributed to a relatively smooth surface (Fig. 3f). The ternary nanocomposite containing both RSN and AgNPs seems to have a more compact structure with homogenous distribution of the nanoparticles. This type of compact structure could be due to relatively greater hydrogen bonding interactions between the constituents in the ternary nanocomposites. AgNPs are known to have excellent interaction with the hydroxyl groups of PVA as well as RSN and thereby acting as bridges between these constituents. These types of interactions can lead to the formation of a discrete, continuous polymer network-like structure, where nanoparticles are uniformly dispersed and distributed. The existence of this type of morphology may be the reason for better properties exhibited by ternary nanocomposites.

## FTIR Analysis of Starch Nanoparticles and Its Nanocomposites

The RS and RSN, extracted from the powdered rice grain were analysed using FTIR spectroscopy, which is shown in Fig. 4A.

The IR frequencies of these samples were found to be matching with other starches reported in the literature [35]. From the figure, it is evident that rice powder is showing a broad IR band, centered around 1534 cm^{-1} which correspond to amide II band of proteins (Fig. 4A—a). After the starch extraction, this band is not visible, which indicates that the proteins have been completely removed from the
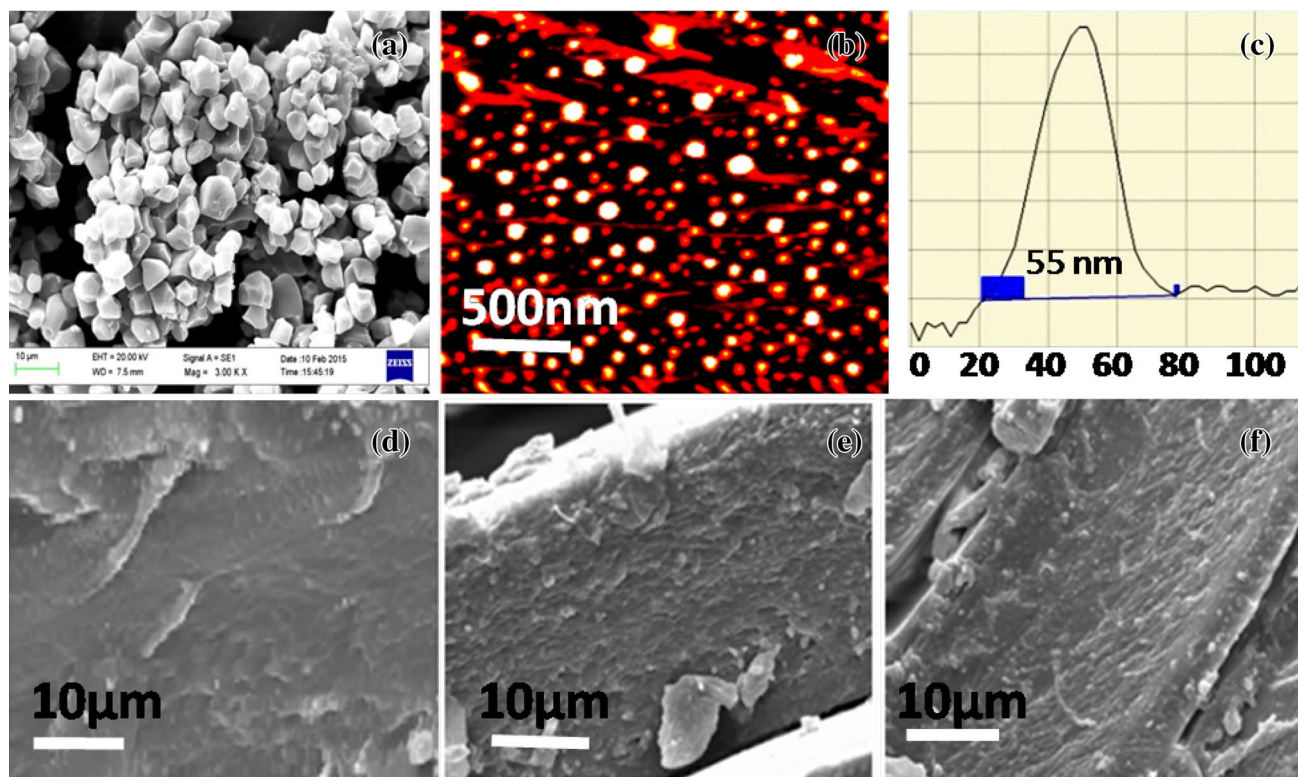
Fig. 3 **a** SEM image of extracted rice starch, **b** AFM image of rice starch nanoparticles, **c** graph showing the size of an individual rice starch nanocrystal, measured using AFM **d** cross sectional view of PVA, **e** cross sectional view of PVA + RSN nanocomposites and **f** cross sectional view of PVA + RSN + AgNPs nanocomposites
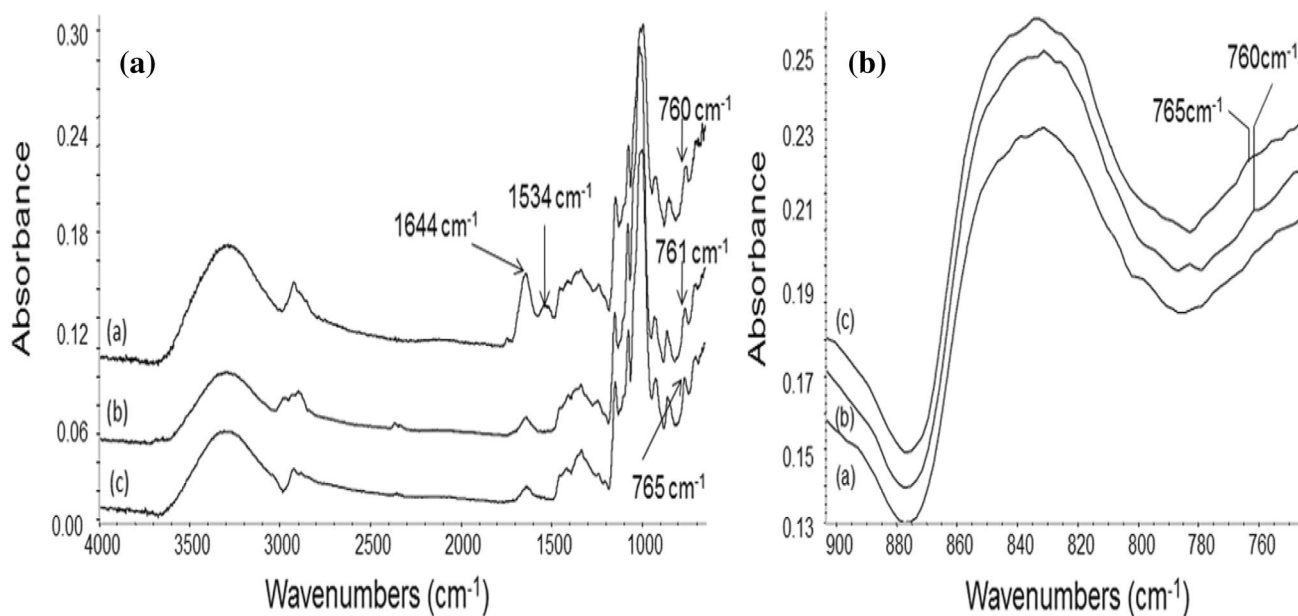

Fig. 4 FTIR spectra of **A** (*a*) raw rice powder, **A** (*b*) extracted rice starch, **A** (*c*) rice starch nanocrystals and **B** (*a*) PVA, **B** (*b*) PVA + RS films and **B** (*c*) PVA + RSN nanocomposites

raw rice powder by alkali method. The strong band appearing at 1644 cm^{-1} for raw rice powder can be assigned to the bending vibration of bound water molecules in it. They exist through a strong hydrogen bonding interaction with starch as well as other polar contents such as proteins in it. After the removal of proteins from raw rice powder, the amount of bound water in the system seems to be reduced and this resulted in decreasing the intensity of this band in RS and RSN. It can also be observed from the figure that the characteristic C–O–C ring vibration of the starch appears at 760 cm^{-1} for raw rice, while it got shifted to 761 and 766 cm^{-1} respectively for RS and RSN. This high-frequency shift of this mode of bending vibration is mainly due to the changes occurring in the interactions of glycosidic linkage and water molecules as a result of alkali treatment. A similar type of observations was also reported in the case of pea starch and pea starch nanoparticles [14]. These bands were also used as a characteristic band of RSN to prove their presence in PVA nanocomposites. The FTIR spectra of RS and RSN containing PVA films where the concentration of PVA + RS and PVA + RSN kept at 8% level are presented in Fig. 4B. The appearance of the characteristic starch band at 761 and 765 cm^{-1} for RS and RSN systems, respectively along with the characteristic bands of PVA confirms the presence of these two starches in the PVA nanocomposite films. PVA has shown its characteristic absorption at 1732 cm^{-1}, which were not overlapped by any other absorption peaks of rice starch. The characteristic bands of PVA and rice starch co-existed in the FTIR spectra confirming the presence of both in the nanocomposite films.

Physico-Mechanical Properties

The stress–strain graph of PVA and its nanocomposite films is given in Fig. 5. The tensile strength and percentage strain at break of each sample are depicted in Table 2. The addition of 8 wt% of RS in PVA reduced the tensile strength and percentage elongation in comparison to PVA (Fig. 5a, b). An increase in the concentration of rice starch in PVA decreased some of the mechanical properties, which reveals that starch is having some limitations in reinforcing PVA, which is in agreement with the reports available elsewhere [36]. This is due to the lack of adequate molecular interactions between PVA and starch, where starch is acting the role of normal filler rather than reinforcing filler. On the other hand, the addition of a similar quantity of starch nanocrystals (8 wt%) to PVA resulted in an increase in the mechanical properties (Fig. 5c).

The reinforcing properties of RSN can be explained on the basis of its nanoscale dimensions, relatively better dispersion within the PVA matrix and H-bonding interaction between the hydrophilic polymer and starch nanocrystals. The possibility of H-bonding between RSN and PVA,
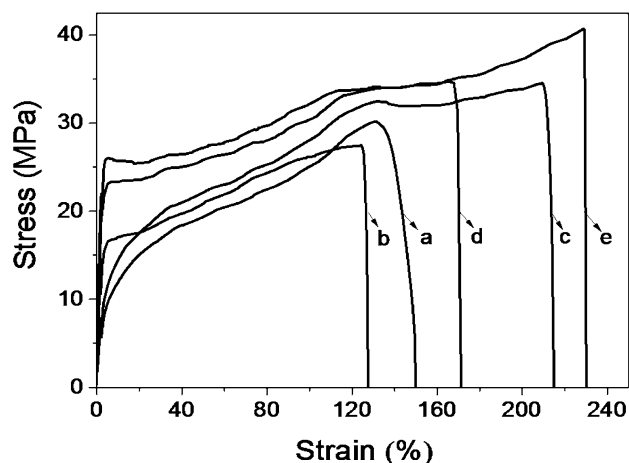
Fig. 5 Stress–strain graph of (*a*) PVA, (*b*) PVA + RS (8 wt%), (*c*) PVA + RSN (8 wt%), (*d*) PVA + RSN (10 wt%) and (*e*) PVA + RSN (8 wt%) + AgNPs films

Table 2 Mechanical properties of PVA and its nanocomposites

Sl No	Samples	Tensile strength (MPa)[a]	Strain at break (%)[a]
1	PVA	30.3 ± 2.6	148.7 ± 18.9
2	PVA + RS (8 wt%)	27.7 ± 2.8	128.7 ± 16.5
3	PVA + RSN (8 wt%)	34.6 ± 3.5	216.8 ± 19.4
4	PVA + RSN (10 wt%)	34.8 ± 2.9	172.3 ± 17.7
5	PVA + RSN (8 wt%) + AgNPs	41.1 ± 3.4	231.2 ± 18.6

[a]Mean ± SE (n = 10)

facilitate easy stress transfer from the polymer matrix to more rigid starch nanoparticles. Thus the starch nanocrystal acts as a load bearing component, which results in improved tensile strength and modulus of the polymer nanocomposites. All these factors contributed to enhancing the mechanical properties at RSN loadings up to 8 wt% level, while a further increase of RSN to 10 wt%, decreased the elongation properties (Fig. 5d). It has been observed that with increasing the concentration of RSN beyond 8 wt% level, the nanocomposite films tend to become brittle. As the concentration of the nano materials in the polymer matrix increases, more and more RSN particles come closer to each other, resulting in molecular interactions among themselves, which can lead to agglomeration of the nano particles or the formation of a 3-dimensional network of self-assembled nanoparticles within the system. Higher concentration of RSN in the polymer matrix resulted in the formation of weak points, which tend to undergo a fracture with lower strain compared to the polymer nanocomposites having a lower concentration of nanomaterials. The fracture developed can spread cracks along the nanocomposite film as it transfers the load through

the nanomaterial to the PVA matrix resulting in the overall failure of the polymer nanocomposite. With an increase in further loading of RSN, self-aggregation occurs and resulted in reduced properties. Similar results were reported where a large concentration of pea starch nanoparticles decreased the mechanical properties of nanocomposite films [14].

The preparation of ternary nanocomposites, where more than one type of reinforcing nanoparticles is used in the same polymer matrix is a viable method to reduce the brittleness of these types of polymer nanocomposites. In the present investigation, silver nanoparticles at lower concentration were used along with starch nanocrystals in PVA to reduce the brittleness problem. The addition of 0.1% AgNPs along with 8% RSN improved the mechanical properties and reduced the brittleness and enhanced strength and modulus as evident from Fig. 5e. AgNPs were prepared in situ by reducing silver nitrate in the presence of PVA, where hydroxyl groups act as capping agents. The hydroxyl groups strongly interact with silver cations, which reduce their mobility and thus stabilises AgNPs. These nanoparticles can also act as a link between various polymer chains through molecular interactions and thereby increase the interfacial adhesion between the polymer matrix and the nanoparticle. Due to a certain type of interaction that exists between rice starch nanocrystals and PVA, the polymer chain mobility is restricted, which resulted in a reduced percentage elongation (Fig. 5b). The presence of much smaller nanoparticles, such as AgNPs can reduce these interactions, as a large number of –OH groups of both polymer and starch nanocrystals can be complexed with AgNPs and will not be available for polymer–starch nanocrystal interactions [37]. This makes the polymer chains relatively free to move and can regain some of the lost elongation properties. The physical cross-link formation between the polymer and nanocrystals within the polymer nanocomposites is responsible for the enhanced strength and modulus of the nanocomposites films.

Differential Scanning Calorimetric Analysis

DSC thermograms of PVA and its nanocomposites are used to calculate the thermal parameters such as T_g and T_m (Fig. 6A). PVA exhibited a T_g at 23.4 °C and T_m at 187.6 °C (Table 3).

The incorporation of RSN into PVA at 4 and 8 wt%, increased the T_g to 24.3 and 26.3 °C respectively as evident from the Fig. 6A—b, c. The glass transition can be influenced by the level of interaction existing between polymer chains and nanocrystals. A better interaction is expected to be present in these nanocomposites as the starch nanocrystals can have hydrogen bonding type interaction with the polymer. Moreover, both the polymer and nanocrystal are hydrophilic in nature and hence are more compatible. This type of interactions can restrict the segmental mobility of
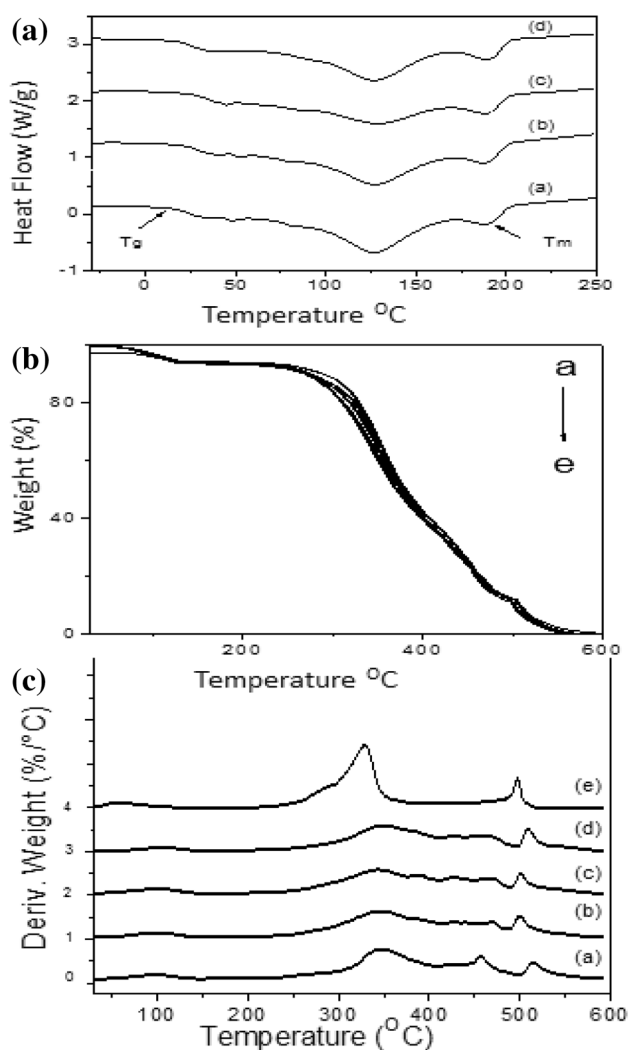
Fig. 6 DSC thermograms **A** of (*a*) PVA, (*b*) PVA+RSN (4 wt%), (*c*) PVA+RSN (8 wt%), (*d*) PVA+RSN (8 wt%)- AgNPs and TGA **B** and DTG (**C**) curves of (*a*) PVA, (*b*) PVA+RSN (4 wt%), (*c*) PVA+RSN (8 wt%), (*d*) PVA+RSN (8 wt%)+AgNPs and (*e*) rice starch nanocrystals

Table 3 DSC data of PVA and its nanocomposites

Samples	Tg (°C)	Tm (°C)	ΔH (J/g)
PVA	23.4	187.6	11.6
PVA+4% RSN	24.3	188.2	12.0
PVA+8% RSN	26.3	189.8	12.8
PVA+8% RSN+0.1%AgNPs	25.1	190.6	13.3

the polymer chain and hence T_g can shift to a higher temperature. The addition of AgNPs slightly reduced the T_g to 25.1 °C, indicating that the presence of AgNPs is affecting the polymer-starch nanocrystal interactions in a different way (Fig. 6A—d). The AgNPs can act as a bridge between

PVA and starch nanocrystals and thereby giving more freedom for the polymer segments to move. This may be the reason for increased flexibility of the film, which was observed from the mechanical property analysis. Other thermal properties, such as T_m and ΔH_m of these nanocomposites have also increased by the addition of the nanocrystals. These results indicate that polymer-nanocrystal interactions are strong and slightly improving the other thermal properties of the nanocomposite films also. The addition of AgNPs also resulted in similar improvement in the properties.

## Thermo Gravimetric Analysis (TGA)

Thermal stability is an important parameter of polymers, as it will help to find out the proper polymer processing temperatures and to avoid their decomposition during thermal processing. The thermal stability of PVA and its nanocomposites were evaluated using TGA and is shown in Fig. 6B. The TGA curves imply that the addition of RSN decreased the thermal stability. In order to have a better understanding, derivative thermograms (DTG) were plotted in the Fig. 6C. The thermal degradation of PVA occurred in different stages as evident from the figure (Fig. 6C—a) and the first stage occurs at a temperature above 300 °C. The decomposition in this range is usually associated with the dehydration of the hydroxyl groups present in the polymer [38]. This is followed by the formation of volatile organic compounds which subsequently produce conjugated unsaturated polyene structures. As temperature increases above 450 °C, the second stage degradation initiates, where low molecular weight compounds such as alkenes, alkanes and aromatics were produced. Above 500 °C, carbonaceous residues will

be formed [39]. In this investigation, it was observed that the addition of RSN slightly reduced the thermal stability of PVA. The DTG curve of RSN alone (Fig. 6C—e) implies that it is less thermally stable than PVA and the early onset of decomposition of RSN can initiate some degradation in PVA. The degradation products emanating from the RSN can induce some amount of early degradation to the polymer matrix also. This may be the reason for the reduced thermal stability of PVA–RSN nanocomposites, and the thermal stability was found to reduce further as the percentage of RSN increased from 4 to 8 wt% (Fig. 6C—b, c). The addition of AgNPs, on the other hand, prevented such early onset of degradation as depicted in Fig. 6C—d, which implies that these metallic nanoparticles are protecting the RSN from early degradation and imparting improved thermal stability to these nanocomposites. Thus, the ternary nanocomposites were found to have better thermal stability than PVA nanocomposites containing only RSN and are almost retaining the original thermal stability of PVA. This also implies that a combination of nanoparticles can be helpful in compensating the drawbacks of a single type of nanoparticle.

Dynamic Mechanical Analysis (DMA)

Dynamic mechanical properties of PVA based nanocomposites were analysed by recording various parameters such as storage modulus and loss tangent as a function of temperature as depicted in Fig. 7a.

The storage modulus of PVA nanocomposites was found to increase considerably after the incorporation of RSN (Fig. 7A—b, c) compared to that of PVA (Fig. 7A—a). This indicates that the presence of RSN played a predominant
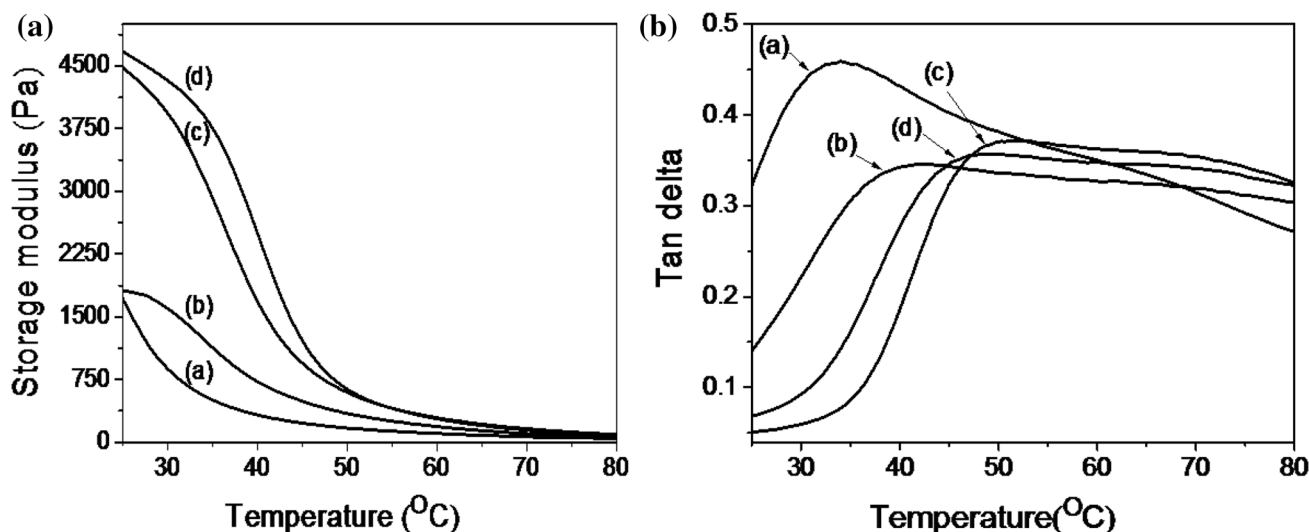
Fig. 7 DMA plots of **A** Modulus versus temperature graphs of (*a*) PVA, (*b*) PVA+RSN (4 wt%), (*c*) PVA+RSN (8 wt%), (*d*) PVA+RSN (8 wt%)+AgNPs and **B** Tan δ versus temperature graphs of (*a*) PVA, (*b*) PVA+RSN (4 wt%), (*c*) PVA+RSN (8 wt%), (*d*) PVA+RSN (8 wt%)+AgNPs

role in improving the dynamic mechanical properties of nanocomposite due to the strong interaction between RSN and PVA. The possible formation of a three-dimensional network like structure can maximize the stress transfer and contribute to the rise in overall modulus of polymer nano-composites. The addition of AgNPs along with RSN further enhanced the storage modulus, which may be due to the fact that AgNPs can act as physical cross links between PVA chains [37]. The tan δ vs temperature peaks (Fig. 7B) exhibited a substantial change in the maximum temperature (T_{max}). The shift in T_{max} towards higher temperature with the addition of RSN indicates an increase in the T_g values of the nanocomposite systems. This correlates well with the trend visible from the DSC studies also. The incorporation of nano fillers such as RSN into PVA matrix resulted in decreased segmental mobility, which in turn resulted in an increased T_g. This also demonstrates a substantial change in the segmental dynamics within the disordered and crystal-line regions of the polymer matrix caused by the presence of starch nanocrystals [40]. But the addition of AgNPs is slightly reducing the T_g as evident from the reduction in T_{max} to lower temperatures (Fig. 7B—d). Thus AgNPs can act as a bridge between PVA and RSN and thereby giving more freedom for the polymer segments to move and ultimately giving more flexibility to these films, which is a desirable property as far as film applications are concerned.

Conclusion

Rice starch, being a natural and low-cost material, prepara-tion of its nanocrystals and employing them for reinforc-ing polymers is a sustainable method for the fabrication of polymer nanocomposites with improved properties. The addition of RSN up to 8 wt% in PVA proved to enhance the mechanical properties such as tensile strength, modu-lus etc. The thermal properties of these nanocomposites were also analysed and it was observed that the addition of RSN significantly increased the Tg values. The addition of a second nanomaterial such as AgNPs resulted in syn-ergistically improving the mechanical properties of PVA Nanocomposites. This may be due to the strong interaction of AgNPs with both PVA and RSN, which resulted in better properties. The small size and better homogeneous disper-sion of AgNPs in PVA matrix are also contributing factors. The addition of AgNPs enhanced the elongation properties, which is an added advantage and also helped to reduce the Tg. This proves that hybrid nanocomposite films with better properties can be prepared by using a combination of two different nanoparticles.

References

1. George J, Sabapathi SN, Siddaramaiah (2015) Water soluble poly-mer-based nanocomposites containing cellulose nanocrystals. In: Thakur VK, Thakur MK (eds) Eco-friendly polymer nanocompos-ites: processing and properties. Springer, Berlin, pp 259–293
2. Tripathi S, Mehrotra GK, Dutta PK (2009) Physicochemical and bioactivity of cross-linked chitosan–PVA film for food packaging applications. Inter J Bio Macromol 45:372–376
3. Paradossi G, Cavalieri F, Chiessi E, Spagnoli C, Cowman MK (2003) Poly(vinyl alcohol) as versatile biomaterial for potential biomedical applications. J Mater Sci 14:687–691
4. Follain N, Joly C, Dole P, Bliard C (2005) Mechanical properties of starch-based materials: I—short review and complementary experimental analysis. J Appl Polym Sci 97:1783–1794
5. Lu J, Wang T, Drzal LT (2008) Preparation and properties of microfibrillated cellulose polyvinyl alcohol composite materials. Compos A 39:738–746
6. Jia YT, Gong J, Gu XH, Kim HY, Dong J, Shen XY (2007) Fabri-cation and characterization of poly (vinyl alcohol)/chitosan blend nanofibers produced by electrospinning method. Carbohydr Polym 67:403–409
7. Su JF, Huang Z, Liu K, Fu LL, Liu HR (2007) Mechanical proper-ties, biodegradation and water vapor permeability of blend films of soy protein isolate and poly (vinyl alcohol) compatibilized by glycerol. Polym Bullet 58:913–921
8. Siddaramaiah, Raj B, Somashekar R (2004) Structure–property relation in polyvinyl alcohol/starch composites. J Appl Polym Sci 91:630–635
9. Xue P, Park KH, Tao XM, Chen W, Cheng XY (2007) Electrically conductive yarns based on PVA/carbon nanotubes. Compos Struct 78:271–277
10. Yang X, Li L, Shang S, Tao XM (2010) Synthesis and characteri-zation of layer-aligned poly (vinyl alcohol)/graphene nanocom-posites. Polymer 51:3431–3435
11. Lee BO, Woo WJ, Kim MS (2001) EMI shielding effectiveness of carbon nanofiber filled poly (vinyl alcohol) coating materials. Macromol Mater Eng 286:114–118
12. Yu YH, Lin CY, Yeh JM, Lin WH (2003) Preparation and proper-ties of poly(vinyl alcohol) clay nanocomposite materials. Polymer 44:3553–3560
13. George J, Bawa AS, Siddaramiah (2010) Synthesis and charac-terization of bacterial cellulose nanocrystals and their PVA nano-composites. Advanc Mater Res 123:383–386
14. Chen Y, Cao X, Chang PR, Huneault MA (2008) Comparative study on the films of poly(vinyl alcohol)/pea starch nanoparti-cles and poly(vinyl alcohol)/native pea starch. Carbohydr Polym 73:8–17
15. Zeng QH, Yu AB, Lu GQ (2008) Multiscale modeling and simula-tion of polymer nanocomposites. Progr Polym Sci 33:191–269
16. Suzuki T, Chiba A, Yarno T (1997) Interpretation of small angle X-ray scattering from starch on the basis of fractals. Carbohydr Polym 34:357–363
17. Jenkins PJ, Donald AM (1997) The effect of acid hydrolyis on native starch granule structure. Starch–Stärke 49:262–267
18. Lin N, Huang J, Chang PR, Anderson DP, Yu J (2011) Prepara-tion, modification, and application of starch nanocrystals in nano-materials: a review. J Nanomater 2011:20

19. Putaux JL, Molina-Boisseau S, Momaur T, Dufresne A (2003) Platelet nanocrystals resulting from the disruption of waxy maize starch granules by acid hydrolysis. Biomacromol 4:1198–1202

20. Wang Y, Zhang L (2008) High-strength waterborne polyurethane reinforced with waxy maize starch nanocrystals. J Nanosci Nanotech 8:5831–5838

21. Namazi H, Dadkhah A (2010) Convenient method for preparation of hydrophobically modified starch nanocrystals with using fatty acids. Carbohydr Polym 79:731–737

22. Bouthegourd E, Rajisha KR, Kalarical N, Saiter JM, Thomas S (2011) Natural rubber latex/potato starch nanocrystal nanocomposites: correlation morphology/electrical properties. Mater Lett 65:3615–3617

23. Zheng H, Ai F, Chang PR, Huang J, Dufresne A (2009) Structure and properties of starch nanocrystal-reinforced soy protein plastics. Polym Compos 30:474–480

24. Angellier H, Molina-Boisseau S, Lebrun L, Dufresne A (2005) Processing and structural properties of waxy maize starch nanocrystals reinforced natural rubber. Macromolecules 38:3783–3792

25. George J, Kumar R, Sajeevkumar VA, Ramana KV, Rajamanickam R, Abhishek V, Nadanasabapathy S (2014) Hybrid HPMC nanocomposites containing bacterial cellulose nanocrystals and silver nanoparticles. Carbohydr Polym 105:285–292

26. Sodi NS, Singh N (2003) Morphological, thermal and rheological properties of starches separated from rice cultivars grown in India. Food Chem 80:99–108

27. Angellier H, Choisnard L, Molina-Boisseau S, Ozil P, Dufresne A (2004) Optimization of the preparation of aqueous suspensions of waxy maize starch nanocrystals using a response surface methodology. Biomacromolecules 5:1545–1551

28. Williams VR, Wu WT, Tasi HY, Bates HG (1958) Varietal differences in amylose content of rice starch. J Agri Food Chem 6:47–48

29. Wani AA, Singh P, Shah MA, Schweiggert-Weisz U, Gul K, Wani IA (2012) Rice starch diversity: effects on structural, morphological, thermal, and physicochemical properties: a review. Compre Rev Food Sci Food Saf 11:417–436

30. Lopez Rubio A, Flanagan BM, Gilbert EP, Gidley MJ (2008) A novel approach for calculating starch crystallinity and its correlation with double helix content: a combined XRD and NMR study. Biopolymers 89:761–768

31. Puchongkavarin H, Bergthaller W, Shobsngob S, Varavinit S (2003) Characterization and utilization of acid-modified rice starches for use in pharmaceutical tablet compression. Starch/Starke 55:464–475

32. McGrance SJ, Cornell HJ, Rix CJ (1998) A simple and rapid colorimetric method for the determination of amylose in starch products. Starch-Stärke 50:158–163

33. Gong B, Liu W, Tan H, Yu D, Song Z, Lucia LA (2016) Understanding shape and morphology of unusual tubular starch nanocrystals. Carbohydr Polym 151:666–675

34. Singh N, Singh J, Kaur L, Sodhi NS, Gill BS (2003) Morphological, thermal and rheological properties of starches from different botanical sources. Food Chem 81:219–231

35. Fang JM, Fowler PA, Tomkinson J, Hill CAS (2002) The preparation and characterisation of a series of chemically modified potato starches. Carbohydr Polym 47:245–252

36. Ramaraj B (2007) Crosslinked poly(vinyl alcohol) and starch composite films: II—physicomechanical, thermal properties and swelling studies. J Appl Polym Sci 103:909–916

37. George J, Sajeevkumar VA, Ramana KV, Sabapathy SN, Siddaramaiah (2012) Augmented properties of PVA hybrid nanocomposites containing cellulose nanoparticles and silver nanoparticles. J Mater Chem 22:22433–22439

38. Peng Z, Kong LX (2007) A thermal degradation mechanism of polyvinyl alcohol/silica nanocomposites. Polym Degrad Stab 92:1061–1071

39. Sin LT, Rahman WA, Rahmat AR, Mokhtar M (2011) Determination of thermal stability and activation energy of polyvinyl alcohol–cassava starch blends. Carbohydr Polym 83:303–305

40. Bershtein VA, Gunko VM, Egorova LM, Wang Z, Illsley M, Voronin EF, Prikhodko GP, Yakushev PN, Leboda R, Skubiszewska-Zieba J, Mikhalovsky SV (2012) Dynamics, thermal behaviour and elastic properties of thin films of poly(vinyl alcohol) nanocomposites. RSC Adv 2:1424–1431